Supporting Information

Computational screening of pyrazine-based graphene supported transition metals as single-atom catalysts for nitrogen reduction reaction

Min Zhang, [a] Caijuan Xia, [a] Lianbi Li, [a] Anxiang Wang, [a] Dezhong Cao, [a] Baiyu Zhang, [b] Qinglong Fang,[a, *] Xumei Zhao [a, *]

[a]*School of Science, Xi'an Polytechnic University, Xi'an 710048, Shaanxi, China*

[b]*Materials Department, University of California, Santa Barbara, California 93106-5050, United States*

* Corresponding authors.

E−mail addresses: qinglong_fang@xpu.edu.cn (Qinglong Fang);

20191211@xpu.edu.cn (Xumei Zhao).

Note S1. Electrochemical durability of the py-GY support.

The durability of materials is investigated because carbon/nitrogen atoms in py-GY may decompose arising from their own nitrogen reduction reaction (NRR) carbon oxidation reaction (COR) and nitrogen oxidation reaction (NOR). During the real NRR process it is thus crucial to evaluate the possibility of substrate decomposition. The process of degradation on py-GY can be defined as follows:

$$C_{32}N_8 + 3H^+ + 3e^- \rightarrow C_{32}N_7 + NH_3(g)$$

$$C_{32}N_8 + H_2O \rightarrow C_{31}N_8 + CO(\mathrm{g}) + 2H^+ + e^-$$

$$C_{32}N_8 + H_2O \rightarrow C_{32}N_7 + NO(\mathrm{g}) + 2H^+ + e^-$$

Therefore, the free energy changes for NRR, COR and NOR can be written as

$$\Delta E_d = E_{C_{32}N_7} + E_{NH_3} - 3E_{(H^+ + e^-)} - E_{C_{32}N_8}$$

$$\Delta E_d = E_{C_{31}N_8} + E_{CO} + 2E_{(H^+ + e^-)} - E_{C_{32}N_8} - E_{H_2O}$$

$$\Delta E_d = E_{C_{32}N_7} + E_{NO} + 2E_{(H^+ + e^-)} - E_{C_{32}N_8} - E_{H_2O}$$

$$\Delta G_d = \Delta E_d + \Delta E_{ZPE} - T\Delta S$$

Where $E_{C_{32}N_8}$, $E_{C_{31}N_8}$ or $E_{C_{32}N_7}$, E_{NH_3}, $E_{(H^+ + e^-)}$, E_{CO}, E_{NO} and E_{H_2O} are the energies of py-GY substrate, decomposed py-GY, NH_3, ($H^+ + e^-$)pair, CO, NO and H_2O, respectively. Therefore, the potential of electrochemical decomposition (U_d) can be given by

$$U_d = -\Delta G_d / ne$$

where n = 3 for NRR, whereas n = 2 for COR and NOR[1].

Note S2. Diffusion energy barrier calculations.

The diffusion energy barriers (G_{bar}) for the TM atom migration from the deposition site to the neighboring site are calculated by CI-NEB[2], the definition of the G_{bar} is defined as follow:

$$G_{bar} = G_{TS} - G_{IS}$$

where G_{IS} and G_{TS} represent the Gibbs free energies of the initial state and transition state respectively. Taking Mo_{II}@py-GY as a representative and its structures of initial (IS) transition (TS) and final (FS) state are plotted in Fig. S9.

Note S3. Synthetic feasibility for Mo_{II}@py-GY in the experiment.

The wet chemical method for the experimental preparation of highly dispersed SACs is a promising approach[3,4]. Inspired by previous theoretical works[5,6], using $MoCl_2$ as the Mo-atom precursor, the experimentally synthetic feasibility of Mo_{II}@py-GY was evaluated by calculating the energy map as the well-designed synthetic route in Fig. S13, as described below:

$$MoCl_2 + * \rightarrow *MoCl_2$$

$$*MoCl_2 + 2H_3O^+ + 2e^- \rightarrow *Mo + 2H_2O \cdot HCl$$

where * represents the py-GY substrate.

Table S1. The binding energy E_b of TM anchored on py-GY at I and II sites, and the transferred charge Q from TM-atoms to substrate at I and II sites.

metal	E_b(I) (eV)	E_b(II) (eV)	Q(I) (e^-)	Q(II) (e^-)
Sc	-4.74	-5.32	1.43	1.49
Ti	-3.72	-5.25	1.23	1.23
V	-4.15	-4.51	1.09	1.11
Cr	-2.61	-3.46	0.89	1.02
Mn	-1.48	-3.08	1.09	0.96
Fe	-3.95	-3.82	0.90	0.81
Co	-3.41	-4.04	0.87	0.57
Ni	-3.34	-4.06	0.51	0.46
Cu	-3.65	-2.59	0.64	0.62
Y	-4.87	-5.49	1.71	2.00
Zr	-5.02	-6.43	1.43	1.53
Nb	-5.31	-6.75	1.16	1.28
Mo	-3.33	-4.36	0.86	0.99
Tc	-4.12	-4.81	1.00	0.77
Ru	-4.21	-4.70	0.63	0.68
Rh	-4.24	-4.28	0.45	0.53
Pd	-3.12	-2.65	0.34	0.28
Ag	-2.46	-2.46	0.53	0.53
Hf	-4.84	-6.33	1.39	1.40
Ta	-4.64	-6.67	1.17	1.36
W	-4.17	-5.46	0.96	1.10
Re	-3.58	-4.37	0.97	0.94
Os	-4.31	-4.90	0.63	0.57
Ir	-4.85	-4.93	0.36	0.43
Pt	-4.73	-4.00	0.18	0.26
Au	-2.99	-1.28	0.41	0.41

Table S2. The adsorption Gibbs free energy E_{abs} and the TM-N and N-N bond lengths of the N_2 adsorption on the TM@py-GY monolayer via end-on and side-on configurations at I site. The "/" means N_2 adsorption configuration changes after structure optimization. The "//" means N_2 physisorption and was not further calculated.

TM	End-on			Side-on			
	E_{abs}(eV)	TM-N(Å)	N-N(Å)	E_{abs}(eV)	TM-N(Å)	TM-N(Å)	N-N(Å)
Sc	-1.16	2.15	1.13	-0.97	2.22	2.22	1.17
Ti	-0.86	2.01	1.14	-0.89	2.01	2.02	1.20
V	-0.86	1.96	1.14	0.07	1.96	1.96	1.20
Cr	0.06	2.05	1.13	/	/	/	/
Mn	-0.44	2.08	1.13	-0.26	1.99	1.99	1.17
Fe	-0.42	1.89	1.13	0.01	2.00	2.05	1.16
Co	-0.33	1.84	1.13	0.18	2.12	2.14	1.14
Ni	-0.15	1.81	1.13	/	/	/	/
Cu	//	//	//	/	/	/	/
Y	-0.60	2.27	1.14	-0.68	2.36	2.36	1.17
Zr	-1.05	2.07	1.15	-1.09	2.10	2.10	1.23
Nb	-0.69	2.03	1.14	-0.76	1.94	1.94	1.29
Mo	-0.39	1.97	1.14	0.06	2.09	2.09	1.19
Tc	-0.66	1.14	1.14	-0.10	2.07	2.07	1.18
Ru	-0.87	1.85	1.14	-0.28	2.08	2.08	1.17
Rh	-0.40	1.87	1.13	0.09	2.16	2.16	1.15
Pd	0.30	2.07	1.12	//	//	//	//
Ag	//	//	//	//	//	//	//
Hf	-0.86	2.03	1.15	-1.07	2.06	2.06	1.24
Ta	-0.99	1.97	1.15	-1.28	1.90	1.90	1.30
W	-0.59	1.91	1.15	-0.19	2.01	2.01	1.23
Re	-0.65	1.86	1.15	0.01	1.95	1.95	1.24
Os	-0.77	1.84	1.14	-0.03	2.08	2.08	1.18
Ir	-0.33	1.83	1.14	0.36	2.13	2.13	1.17
Pt	0.67	2.04	1.13	//	//	//	//
Au	//	//	//	//	//	//	//

Table S3. The adsorption Gibbs free energy E_{abs} and the TM-N and N-N bond lengths of the N_2 adsorption on the TM@py-GY monolayer via end-on and side-on configurations at II site. The "/" means N_2 adsorption configuration changes after structure optimization. The "//" means N_2 physisorption and was not further calculated.

TM	End-on			Side-on			
	E_{abs}(eV)	TM-N(Å)	N-N(Å)	E_{abs}(eV)	TM-N(Å)	TM-N(Å)	N-N(Å)
Sc	-0.16	2.35	1.12	-0.39	2.22	2.22	1.17
Ti	-0.56	2.02	1.14	-0.35	2.27	2.20	1.16
V	-0.51	1.95	1.13	0.21	2.32	2.20	1.14
Cr	0.70	1.83	1.14	/	/	/	/
Mn	0.07	2.18	1.12	/	/	/	/
Fe	-0.20	1.92	1.13	0.21	2.00	2.05	1.15
Co	-0.18	1.85	1.13	/	/	/	/
Ni	-0.32	1.83	1.13	/	/	/	/
Cu	0.01	1.94	1.12	/	/	/	/
Y	-0.51	2.32	1.13	-0.37	2.37	2.36	1.17
Zr	-0.46	2.23	1.13	-0.34	2.28	2.26	1.17
Nb	-0.63	2.04	1.14	-0.47	2.09	2.09	1.21
Mo	-0.54	1.93	1.15	0.16	2.14	2.12	1.18
Tc	-0.86	1.85	1.14	0.28	2.17	2.13	1.17
Ru	-0.19	1.99	1.13	/	/	/	/
Rh	0.42	1.99	1.13	//	//	//	//
Pd	0.01	2.06	1.12	//	//	//	//
Ag	0.26	3.21	1.12	//	//	//	//
Hf	-0.45	2.16	1.14	-0.37	2.23	2.20	1.18
Ta	-0.65	2.01	1.15	-0.59	2.05	2.05	1.23
W	-0.79	1.92	1.15	-0.14	2.12	2.07	1.20
Re	-1.08	1.86	1.15	0.12	2.16	2.10	1.18
Os	-0.26	1.90	1.14	/	/	/	/
Ir	0.28	3.20	1.12	//	//	//	//
Pt	-0.11	2.01	1.13	//	//	//	//
Au	0.29	2.15	1.12	//	//	//	//

Table S4. Gibbs free energy changes of ΔG(*O), ΔG(*OH), ΔG(*O + H^+ + e^- → *OH), and ΔG(*OH + H^+ + e^- → *+H_2O) on W_I@py-GY and Mo_{II}@py-GY. The bold numbers represent the maximum free energy change.

Catalysts	ΔG(*O)	ΔG(*OH)	ΔG(*O + H^+ + e^- → *OH)	ΔG(*OH + H^+ + e^- → *+H_2O)
	eV	eV	eV	eV
W_I@py-GY	-1.56	-1.04	0.52	**0.59**
Mo_{II}@py-GY	-0.84	-0.52	0.31	**0.52**

Table S5. Formation energy values of W_I@py-GY and Mo_{II}@py-GY.

Catalyst	E_{form} (eV)	Ref.
W_I@py-GY	-1.10	this work
Mo_{II}@py-GY	-2.13	this work
Fe/N-G	2.26	[7]
Co/N-G	2.27	[8]
Pt/g-C_3N_4	2.88	[9]

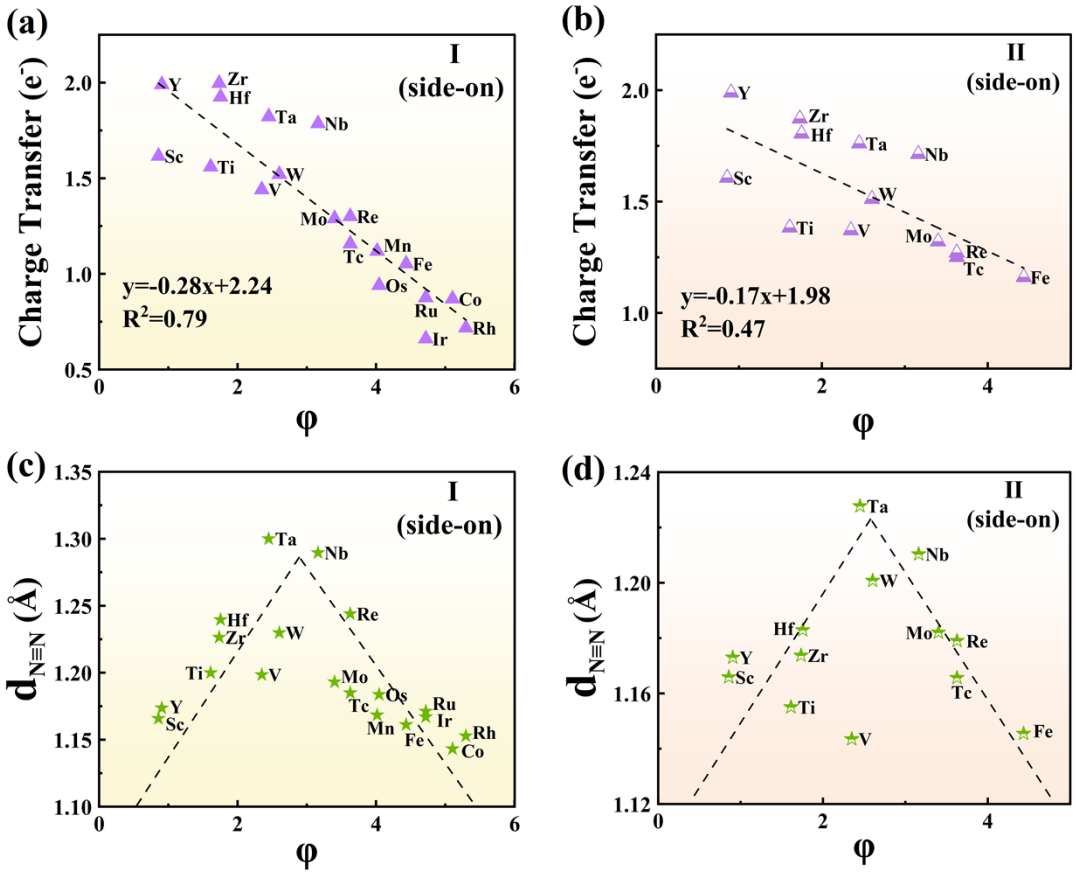

Fig. S1. The linear relationship between the descriptor φ and charge transfer from the metal to N_2 adsorption via the side-on configuration at (a) I and (b) II sites. Relationships between the descriptor φ versus the bond length of N≡N ($d_{N\equiv N}$) at (c) I and (d) II sites.

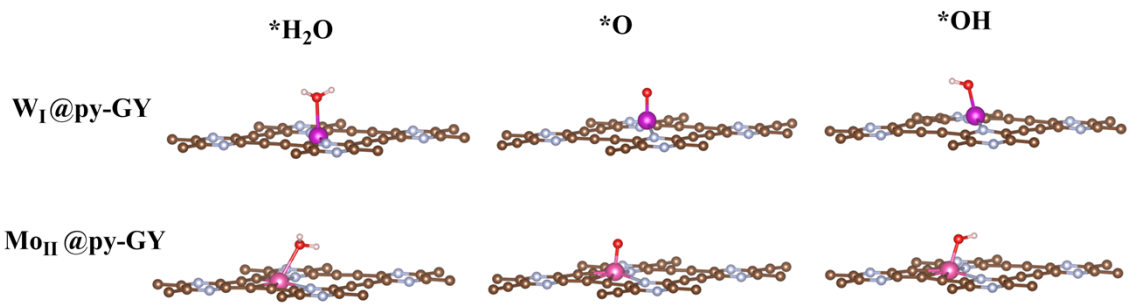

Fig. S2. Optimizated structures of *H_2O, *O, and *OH adsorption on W_I@py-GY and Mo_{II}@py-GY catalysts.

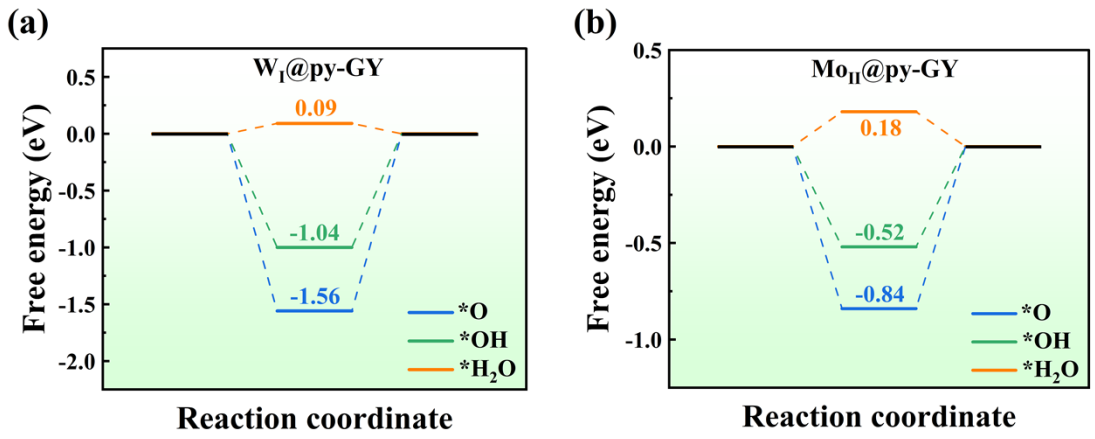

Fig. S3. The Gibbs free energy diagram of *H_2O, *O and *OH adsorption on (a) W_I@py-GY and (b) Mo_{II}@py-GY.

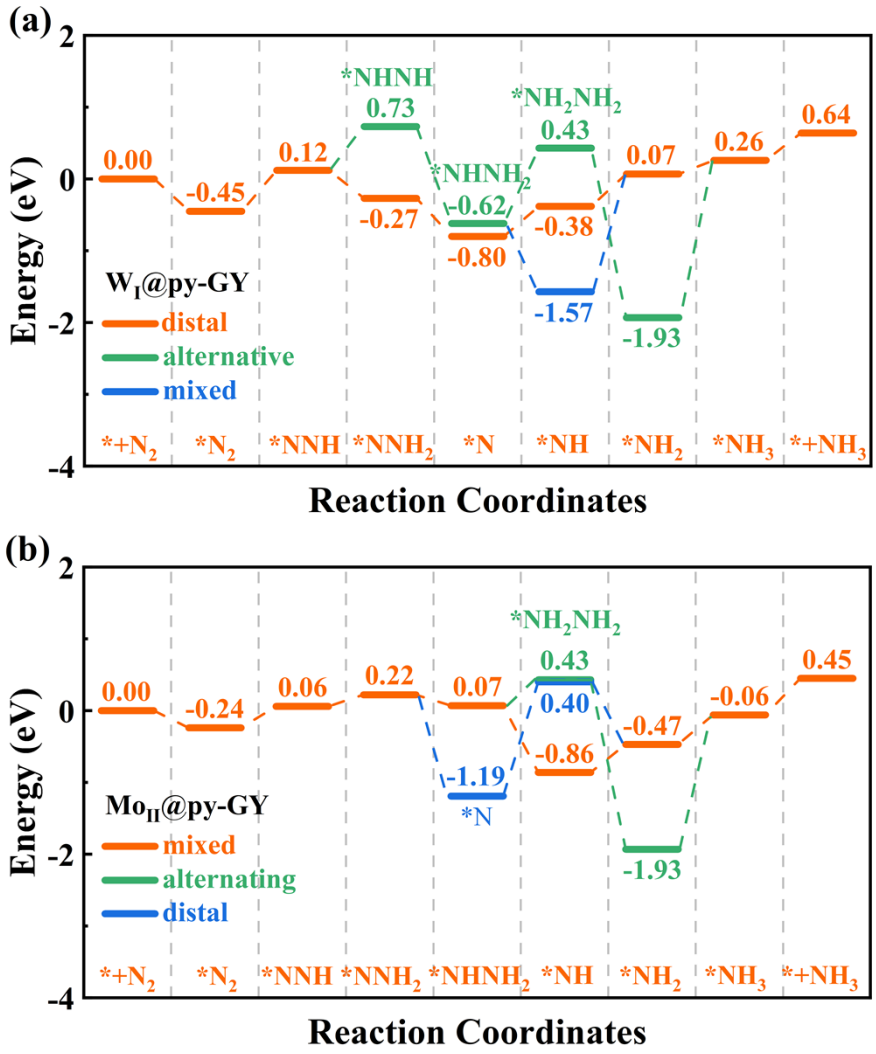

Fig. S4. Free-energy profiles of NRR at different applied potentials on (a) W_I@py-GY , and (b) Mo_{II}@py-GY.

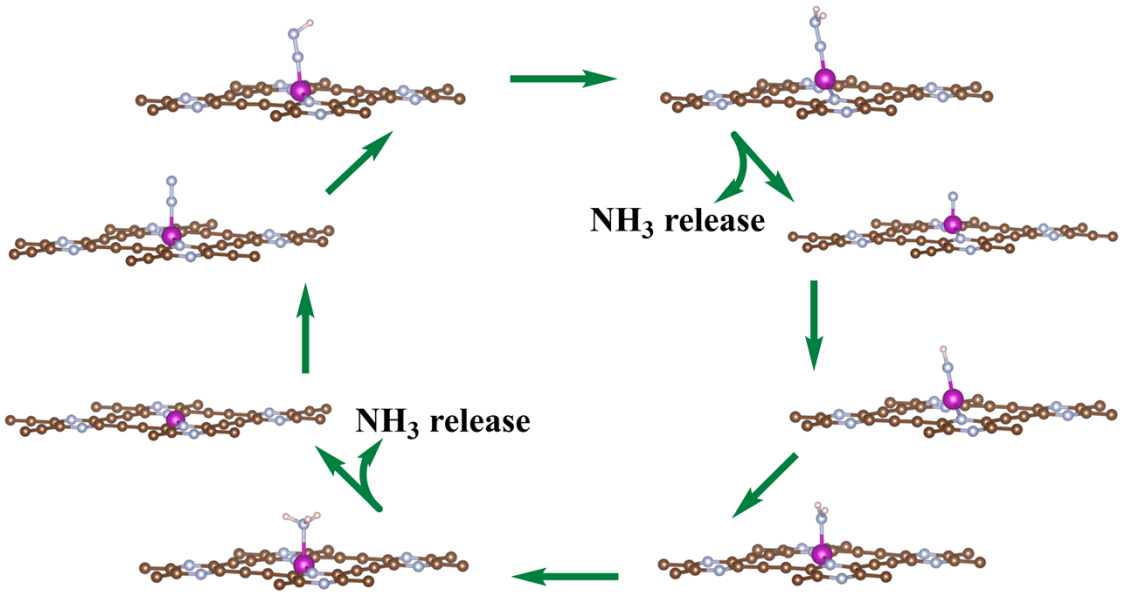

Fig. S5. Adsorption configurations of different species during the reaction on W_1@py-GY surface.

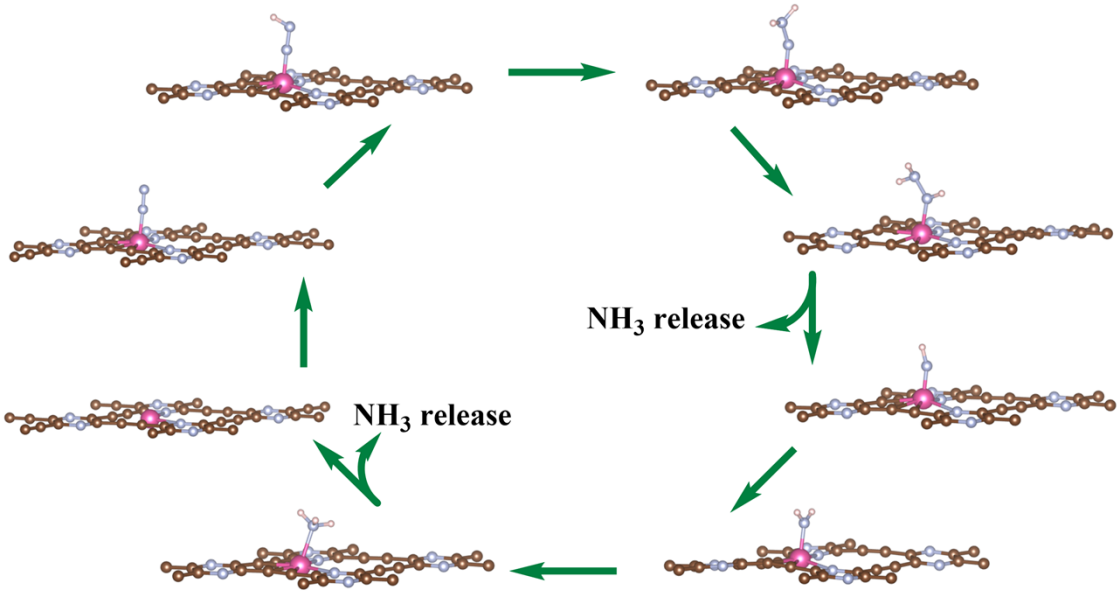

Fig. S6. Adsorption configurations of different species during the reaction on Mo_{II}@py-GY surface.

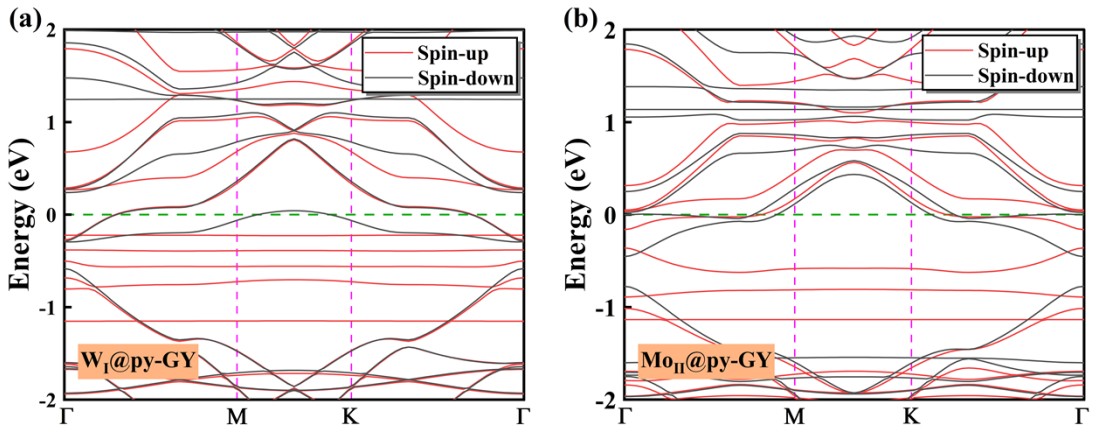

Fig. S7. Band structures of (a) W_I@py-GY and (b) Mo_{II}@py-GY.

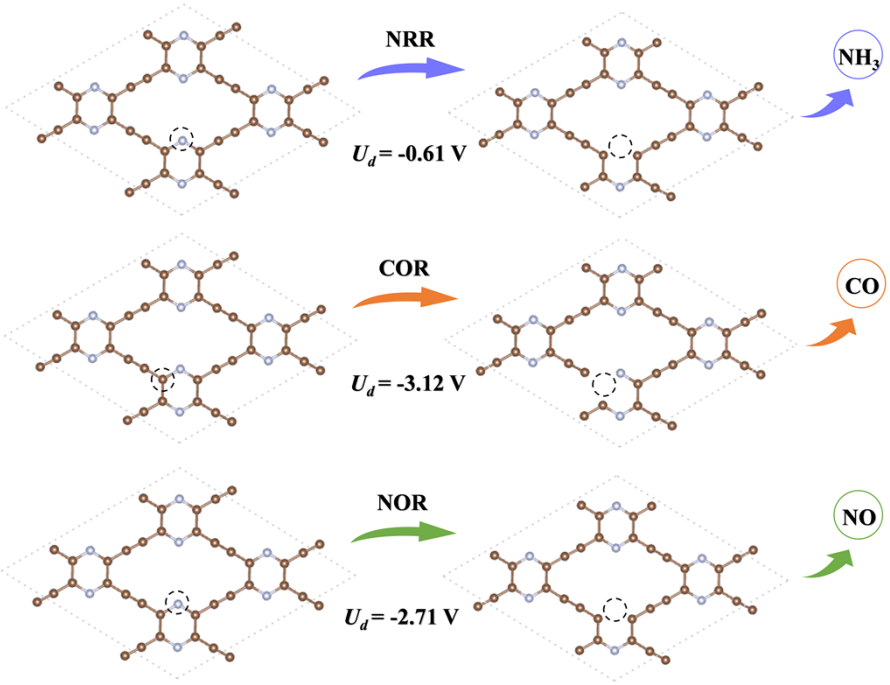

Fig. S8. The required potentials of electrochemical decomposition for nitrogen reduction reaction (NRR) carbon oxidation reaction (COR) and nitrogen oxidation reaction (NOR) on py-GY.

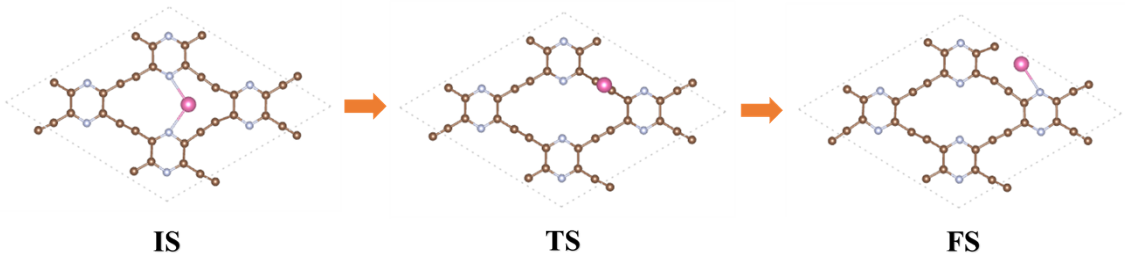

Fig. S9. The atomic structures of the initial state (IS) transition state (TS) and final state (FS) during the TM-atom migration from the deposition site to the neighboring site taking Mo_{II}@py-GY as an example.

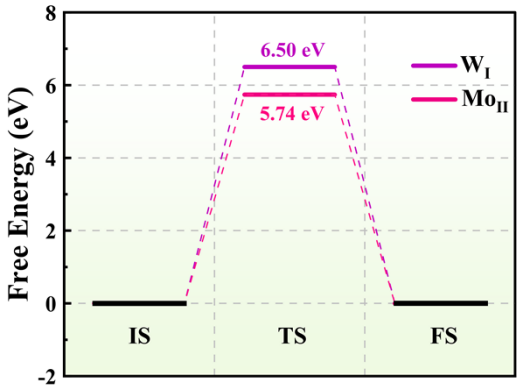

Fig. S10. Diffusion energy barriers of W_I, Mo_{II} from the deposition site of py-GY to neighboring site.

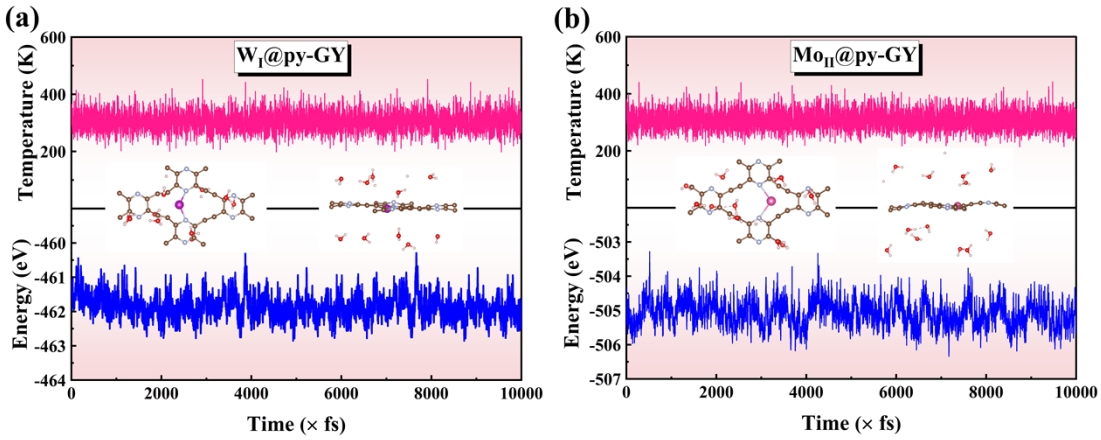

Fig. S11. Energy fluctuations of (a) W_I@py-GY and (b) Mo_{II}@py-GY against the time in AIMD simulations at 300 K. To simulate the acidic aqueous solution, the explicit solvent model (about two H_2O layers) is used and two H atoms are added simulate the acidic aqueous solution.

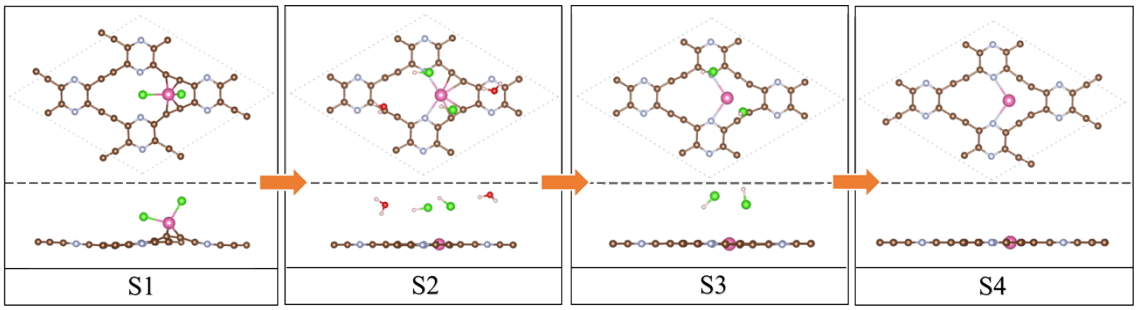

Fig. S12. The designed synthetic route for Mo_{II}@py-GY. Green and red atoms correspond to Cl and O atoms, respectively.

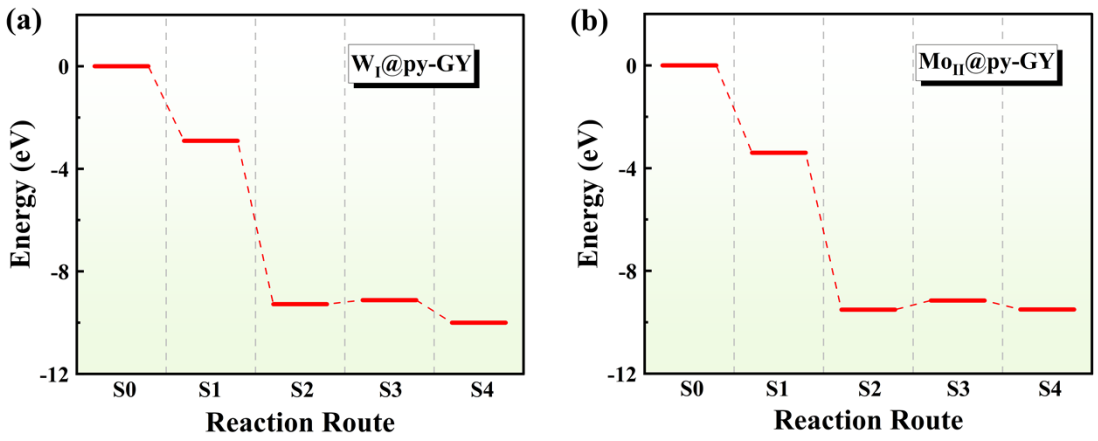

Fig. S13. The energy map along the synthetic route, where S0 denotes the pristine py-GY.

References

[1] X. Lv, W. Wei, H. Wang, B. Huang and Y. Dai, Appl. Catal., B., 2020, 264, 118521.

[2] J. Wu, J.-H. Li and Y.-X. Yu, ACS Appl. Mater. Interfaces, 2021, 13, 10026–10036.

[3] B. Qiao, A. Wang, X. Yang, L. F. Allard, Z. Jiang, Y. Cui, J. Liu, J. Li and T. Zhang, Nat. Chem., 2011, 3, 634–641.

[4] X.-F. Yang, A. Wang, B. Qiao, J. Li, J. Liu and T. Zhang, Acc. Chem. Res., 2013, 46, 1740–1748.

[5] X. Lv, W. Wei, B. Huang, Y. Dai and T. Frauenheim, Nano Lett., 2021, 21, 1871–1878.

[6] C. Ling, L. Shi, Y. Ouyang, X. C. Zeng and J. Wang, Nano Lett., 2017, 17, 5133–5139.

[7] D. Deng, X. Chen, L. Yu, X. Wu, Q. Liu, Y. Liu, H. Yang, H. Tian, Y. Hu, P. Du, R. Si, J. Wang, X. Cui, H. Li, J. Xiao, T. Xu, J. Deng, F. Yang, P. N. Duchesne, P. Zhang, J. Zhou, L. Sun, J. Li, X. Pan and X. Bao, Sci. Adv., 2015, 1, e1500462.

[8] H. Fei, J. Dong, M. J. Arellano-Jiménez, G. Ye, N. Dong Kim, E. L. G. Samuel, Z. Peng, Z. Zhu, F. Qin, J. Bao, M. J. Yacaman, P. M. Ajayan, D. Chen and J. M. Tour, Nat. Commun., 2015, 6, 8668.

[9] Z. Li, M. Li, J. Yang, M. Liao, G. Song, J. Cao, F. Liu, Z. Wang, S. Kawi and Q. Lin, Catal. Today, 2022, 388–389, 12–25.